THE PENNSYLVANIA STATE UNIVERSITY
SCHREYER HONORS COLLEGE

DEPARTMENT OF MECHANICAL ENGINEERING

# SELF-PROPAGATING CHEMICAL-LOOPING COMBUSTION OF SOLID CARBON FUEL WITH COPPER OXIDE

JARRED G. VASINKO
SPRING 2021

A thesis
submitted in partial fulfillment
of the requirements
for a baccalaureate degree
in Mechanical Engineering
with honors in Mechanical Engineering

Reviewed and approved* by the following:

Richard Yetter
Professor of Mechanical Engineering
Thesis Supervisor

Bo Cheng
Professor of Mechanical Engineering
Honors Adviser

* Signatures are on file in the Schreyer Honors College.

## ABSTRACT

Coal is an extremely important fossil fuel for energy production throughout the United States and the world. However, burning coal and other fossil fuels is known to emit harmful greenhouse gases such as carbon dioxide ($CO_2$) into the atmosphere. Carbon capture and storage (CCS) is a leading method for reducing $CO_2$ emissions during energy production, but many current commercial $CO_2$ capturing technologies are energy and cost intensive. Chemical-looping combustion (CLC) is a suggested method for producing a sequestration-ready $CO_2$ stream from the combustion of fossil fuels by using a metal oxide to transport oxygen from the air to the fuel. CLC is a highly researched topic with numerous proposed fuels, metal oxides, and reactor designs. Previous studies have shown that with an externally heated reactor, the combustion of a solid fuel with copper oxide can occur through oxygen uncoupling and solid-solid reaction mechanisms. However, if a hot-spot is produced in a packed mixture of carbon fuel and copper oxide, the reaction may combust rapidly and become self-propagating.

The goal of this study is to test this self-propagating reaction in order to better understand the combustion reaction of solid carbon fuel with copper oxide and to evaluate it as a feasible approach to CLC. The carbon fuel – copper oxide combustion reaction is modeled in a quartz tube under an initial preheat temperature with a laser igniting the reaction and the resulting flame propagation captured on a high-speed camera. The preheat temperature is varied in order to understand the impact of reactant initial temperature on flame propagation and intensity. A higher preheat temperature is shown to increase the flame front coherence and propagation speed. Multiple particle sizes are also tested, with the larger particle sizes producing significantly slower propagations and less coherent flame fronts. Two oxidation states of copper oxide are experimented with to observe the behavior exhibited by different stages of the reaction.

# TABLE OF CONTENTS

LIST OF FIGURES ..... iii

LIST OF TABLES ..... iv

ACKNOWLEDGEMENTS ..... v

Chapter 1 Introduction ..... 1

1.1 Motivation ..... 1
1.2 Introduction to Chemical-Looping Combustion ..... 2
1.3 Selection of an Oxygen Carrier ..... 4
1.4 Chemical-Looping Combustion for Solid Fuels ..... 5
1.5 Solid-Solid Combustion of C-CuO ..... 8
1.6 Post-Combustion Oxidation of Copper ..... 10
1.7 Research Goal and Objectives ..... 12

Chapter 2 Experimental Methods ..... 14

2.1 Copper Oxide Sample Preparation ..... 14
2.2 Combustion Experimental Setup ..... 17

Chapter 3 Results and Discussion ..... 19

3.1 Influence of Preheat Temperature ..... 19
3.2 Influence of Particle Size ..... 24
3.3 Influence of Oxidation State ..... 28

Chapter 4 Conclusion and Future Work ..... 32

Appendix A Images of Experimental Materials, Equipment, and Setup ..... 34

Appendix B Experiment Standard Operating Procedures ..... 36

BIBLIOGRAPHY ..... 41

# LIST OF FIGURES

Figure 1. Diagram of the CLC concept....3

Figure 2. Schematic of the CLOU process compared to the iG-CLC process for solid fuel CLC [11]....6

Figure 3. Reduction reaction performance of CuO with solid fuels [15]....8

Figure 4. TGA profile of combustion reaction of carbon with CuO and $Cu_2O$ [15]....9

Figure 5. Final conversion against temperature for oxidation of Cu to CuO at 1.3 vol% $O_2$ [18] 11

Figure 6. Schematic of combustion reaction experimental setup ....18

Figure 7. Image frames of nano-CuO/C combustion propagation preheated to 400ºC....19

Figure 8. Distance vs. time plot of nano-CuO/C preheated to 400ºC ....20

Figure 9. Nano-CuO/C mixture reaction preheated to 400ºC (a) and preheated to 150ºC (b) .21

Figure 10. Propagation speed vs. preheat temperature of nano-particle CuO/C combustion ..23

Figure 11. Nano-CuO/C combustion (a) and micro-CuO/C combustion (b) both preheated to 400ºC....25

Figure 12. Average propagation speed of micro-particle and nano-particle CuO/C ....26

Figure 13. Auto-ignited samples of microparticle CuO/C (a) and nanoparticle CuO/C (b) ....27

Figure 14. Image of the post combustion products from the CuO/C self-propagation reaction 29

Figure 15. Products of $Cu_2O$/C reaction when auto-ignited (a) and when quenched (b)....31

Figure 16-A. Images of raw CuO (a), Carbon 120 (b), and $Cu_2O$ (c) particles ....34

Figure 17-A. Image of combustion reaction experimental setup....34

Figure 18-A. Image of camera and open preheating furnace with sample ....35

Figure 19-A. Image of sample ignition laser and camera controlling computer....35

# LIST OF TABLES

Table 1. Metal Oxide Properties .....14

Table 2. 105 mm Nikkor and Streampix 6 camera settings. .....17

Table 3. Summary of important metrics for different oxidizers .....33

# ACKNOWLEDGEMENTS

I would first like to thank Dr. Richard Yetter and Dr. Eric Boyer for allowing me to join their combustion research and for guiding me throughout my thesis writing process. Dr. Yetter and Dr. Boyer introduced me to the topic of chemical-looping combustion and I would not have been able to complete this thesis without their support and technical guidance. I would also like to thank my honors advisor, Dr. Bo Cheng, and the Schreyer Honors College for providing me with the opportunity to pursue this research and for their support throughout my thesis writing process. Lastly, I would like to thank my family for supporting me through all of my endeavors and for teaching me the work ethic that has made my achievements possible.

# Chapter 1 Introduction

## 1.1 Motivation

Coal is an extremely important fossil fuel for energy production throughout the United States and the world. However, burning coal and other fossil fuels is known to have adverse effects on the environment, most notably the emission of greenhouse gases into the atmosphere. Carbon dioxide ($CO_2$) is the primary man-made greenhouse gas emitted into the atmosphere through energy production and is a main culprit of climate changes. While alternative energy sources such as wind and solar are gaining popularity to reduce $CO_2$ emissions, the majority of the world remains dependent on fossil fuels for energy generation [1]. Thus, it is highly desirable to develop methods of effectively mitigating or eliminating $CO_2$ emissions in fossil fuel combustion.

Among these mitigation efforts, carbon capture and storage (CCS) remains a key technology. CCS is a post-combustion process that reduces emissions by removing $CO_2$ from the combustion product stream before entering the atmosphere and storing the $CO_2$ where it will not be released. However, the CCS process is complicated by the need to separate $CO_2$ from other gases that are present in the fuel-air combustion product stream, mainly $N_2$ and $NO_x$ gases [2]. A basic conventional combustion process consists of a carbon-based fuel reacting with heat and air to form carbon dioxide, nitrogen gas, water vapor, and energy in the form of heat, as shown by equation (1).

$$Heat + C_nH_m + Air(N_2, O_2) \rightarrow CO_2 + H_20 + N_2 + Heat \quad (1)$$

For the $CO_2$ to be captured and stored, it must first be "scrubbed" away from the other products in the stream, the most difficult to scrub being nitrogen. This complication causes the carbon capture process to be energy and cost intensive [2]. One method of extracting the carbon dioxide for CCS is by combusting fuels with pure oxygen rather than air, creating a flue gas consisting primarily of carbon dioxide and water vapor. With only $H_2O$ and $CO_2$ in the product stream, the $H_2O$ can easily be condensed out, leaving a sequestration-ready $CO_2$ not diluted by $N_2$. By combusting fuels with pure oxygen, $CO_2$ can be separated without the need to extract other gases present during traditional combustion with air.

### 1.2 Introduction to Chemical-Looping Combustion

A conventional oxy-fuel combustion process would require the use of cryogenic air separation to extract pure oxygen. The cryogenic air separation process consumes an appreciable amount of energy, making a conventional oxy-fuel combustion process energy and cost intensive. One alternative method of achieving an oxy-fuel combustion is through chemical-looping combustion (CLC). The CLC process utilizes a solid metal oxide as an oxygen carrier to supply oxygen for the conversion of fuel, similar to the role of hemoglobin within the bloodstream. When a gaseous or solid carbon-based fuel is combusted with the metal oxide, the products stream consists of $CO_2$, $H_2O$, and a reduced solid metal, as shown by reaction (2). The reduced metal is then re-oxidized with air in an external oxidation reactor through reaction (3), resulting in depleted air and regeneration of the metal oxide.

$$C_nH_m + Me_xO_y \rightarrow CO_2 + H_20 + Me_xO_{y-1} \quad (2)$$

$$Me_xO_{y-1} + Air\ (N_2, O_2) \rightarrow Me_xO_y + Depleted\ Air\ (N_2, O_2) \quad (3)$$

The loop is completed when the oxidizer is recirculated into the fuel reactor and is once again combusted with fuel. With the solid reduced metal extracted, the gaseous fuel reactor product stream consists of carbon dioxide and water vaper, with $H_2O$ easily condensed out, leaving a pure stream of $CO_2$. The fuel reactor products stream is isolated from the air reactor, preventing the $N_2$ and other gases within the air from contaminating the $CO_2$ stream or the combustion process. Some of the exhaust gases may also be recirculated to regulate the reactor temperature. The overall CLC process is shown graphically by figure 1 with a general metal oxide, $Me_yO_x$, combusting with a hydrocarbon fuel, $C_nH_m$.

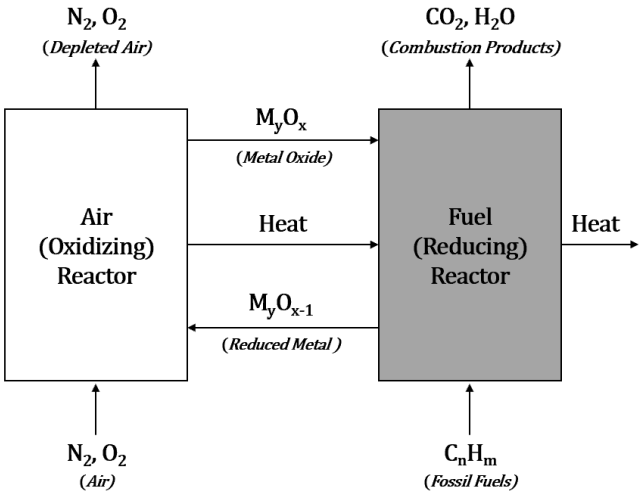


**Figure 1. Diagram of the CLC concept**

The significant advantage of CLC over conventional combustion is that the use of a metal oxide to transport oxygen avoids direct contact between the air and the fuel. This separation produces a stream of sequestration-ready $CO_2$, free of $N_2$ dilution, without the major energy

expenditures of other oxy-fuel reaction methods or traditional carbon separation. Similar to traditional energy production, the heat output from the CLC process can be used to expand a working fluid through a turbine and run a generator.

### 1.3 Selection of an Oxygen Carrier

The oxidation reaction (3) in the air reactor is always exothermic and produces a heat output that can be used for power generation. Depending on the metal oxide used, reaction (2) within the fuel reactor may also be exothermic, as with CuO, $Mn_2O_3$, and $Co_3O_4$, or the reaction may be endothermic, as with NiO, $Fe_2O_3$, and $MoO_3$. The selection of the oxygen carrier is a key aspect of the CLC system's performance. According to Adánez et al. [3], a suitable oxygen carrier for CLC must have a high selectivity towards $CO_2$ and $H_2O$, a suitable oxygen transport capacity, a high reactivity for reduction and oxidation reactions, suitable mechanical strength, negligible agglomeration (good fluidization), and be environmentally and economically feasible. An oxygen carrier is typically composed of a metal oxide that stores and transports oxygen and an inert binder to add mechanical strength and increase fluidization.

Potential metal oxides include Fe, Ni, Cu, Mn, and Co-based molecules, and many studies have been conducted to develop these carriers and determine the most suitable for CLC. Research by Diego et al. [4] showed the importance of adding an inert binder to the metal oxide through significant increases in oxidation rate and maximum conversion rate with the addition of an inert binder. A study by Adánez et al. [5] analyzed 240 metal oxide samples consisting of different metals, concentrations, and binders for their mechanical strength and reactivity during reduction and oxidation. The study determined that Cu-based oxygen carriers (sintered at 950ºC

with $SiO_2$ or $TiO_2$ inerts) and Fe-based carriers (prepared with $Al_2O_3$ and $ZrO_2$ inerts) showed the best behavior based on reactivity and mechanical strength. The study also determined that as the sintering temperature was increased, the reaction rate generally decreased. Through these studies, current front runners for CLC metal oxides include CuO, NiO, $Co_3O_4$, and $Fe_2O_3$ and the performance as an oxygen carrier is dependent on factors such as fuel type and reactor temperature/type. Ilmenite has also been studied as a more natural oxygen carrier because of its low cost and easy access [6]. A study by Cao and Pan [7] determined that among the potential metal oxides, Cu, Ni, and Co-based oxygen carriers are optimal for use in solid fuel CLC and that among these, Cu-based carriers are the only molecules that reduction is autothermal, eliminating the need for external heat in the fuel reactor. From this prior research, copper oxide was identified as a well-suited oxygen carrier for solid fuel CLC.

### 1.4 Chemical-Looping Combustion for Solid Fuels

Currently, the majority of studies have focused on CLC for gaseous fuels, including synthesis gas derived from coal, however fewer studies have been published on the direct use of solid fuels. Development of CLC for solid fuels, especially coal, is desirable because of the intensive use of coal as a fuel within energy production and because coal produces significantly more emissions than other fuels, such as natural gas. Different methods for utilizing solid fuels in CLC have been proposed and studied. Some methods include gasification of the solid fuel either before entering the reactor (Syngas-CLC) or inside of the fuel reactor (iG-CLC) [3], [8]–[10]. The Syngas-CLC process involves gasifying the solid fuel particles before entering the CLC system, creating a syngas fuel to react with the oxygen carrier. In-situ Gasification (iG-CLC)

avoids the external gasification by reacting the metal oxide with the fuel gasification products directly in the CLC system. However, both of these methods show that the gasification reaction is the rate limiting step, which is much slower than the metal oxide reaction, and the reaction must occur at high temperatures. Gasification methods also have a high potential for leaving unburnt fuel which can exit the fuel reactor and possibly burn in the air reactor, producing uncaptured $CO_2$ [8]. Because of these known issues with the gasification CLC methods, it is desirable to develop methods that eliminate the need for gasification of the solid fuel.

One method to eliminate the gasification process is through chemical-looping with oxygen uncoupling (CLOU). The CLOU process utilizes metal oxides with oxygen uncoupling capabilities that allow them to release gaseous oxygen in the fuel reactor to react with the fuel and create an oxygen-fuel combustion, eliminating the need for fuel gasification. Char and volatile matter are burnt by oxygen as with conventional combustion, leading to improved fuel conversion and higher $CO_2$ capture efficiency in CLOU over iG-CLC [11]. Figure 2 shows a schematic of the iG-CLC method compared to the CLOU method where the oxygen carrier generates gaseous oxygen which reacts with the fuel char and volatiles.

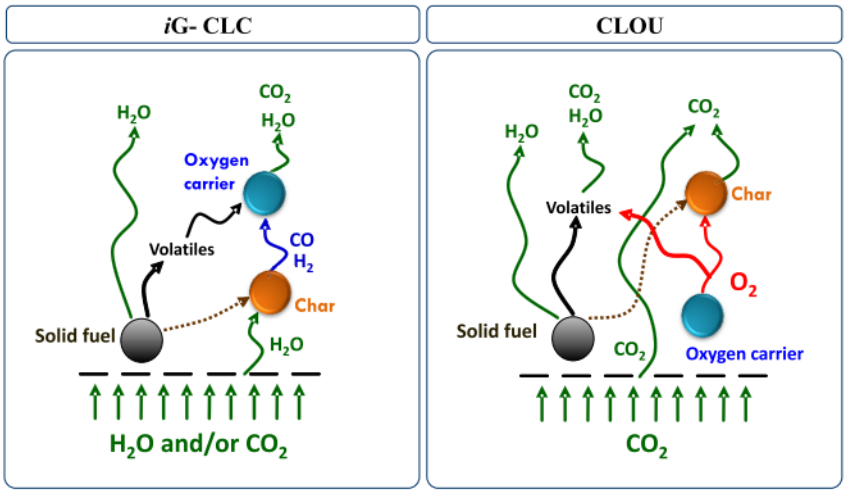


**Figure 2. Schematic of the CLOU process compared to the iG-CLC process for solid fuel CLC** [11].

A study by Mattison et al. [12] showed the feasibility of CLOU with conversion rates a factor of 50 higher than gasification CLC methods. The CLOU process requires the use of oxygen carriers that can both release gaseous oxygen in the fuel reactor and capture and hold oxygen in the air reactor. Copper oxide was identified as a possible metal oxide that meets the requirements of CLOU as it can capture and release oxygen in the gas phase through the reversible reaction shown in (4).

$$4CuO \leftrightarrow 2Cu_2O + O_2(g) \quad \Delta H_{850} = 263.2kJ/mol\ O_2 \tag{4}$$

A potential downfall of the CLOU process is that it is designed for high enough temperatures (typically above 800ºC) for the oxygen uncoupling step to occur. The reaction mechanism also still contains a limiting gas phase intermediate and other methods propose further simplifying the process by reacting the metal oxide directly with the fuel via a solid-solid reaction. Siriwardane et al. [13] analyzed the possibility of this reaction mechanism and showed that CuO reacts with solid carbon fuel via a "fuel-induced oxygen release" in a solid-solid reaction, avoiding the need for gaseous intermediates such as CO and $CO_2$ used in CLOU and other solid fuel processes. Cao and Pan [7], [14] examined the overall CLC process with solid fuels and the reaction of CuO with coal using a simultaneous thermal analyzer to measure heat flow and mass loss of the sample. The thermodynamic analysis indicated that a $CO_2$ concentration above 99% could be achieved through a solid-solid CLC reaction. These studies show that it is possible to achieve solid fuel CLC without gasification through a solid-solid reaction with carbon fuel and CuO.

### 1.5 Solid-Solid Combustion of C-CuO

Another study by Siriwardane et al. [15] analyzed the mechanisms of the solid-solid reaction between a solid carbon fuel and copper oxide. This study showed that the C/CuO and Cu/air reactions take place at lower temperatures (as low as 500ºC) while maintaining useful reaction rates. Contact points between the fuel and the oxidizer particles are critical for the low temperature reaction to occur. TGA results showed that CuO reacts with carbon at a significant rate around 480ºC and similarly, CuO combusts with coal char at 779ºC with an even higher reaction rate, as shown in figure 3. Because carbon and char fuels do not produce volatiles when heated, this data indicates that volatiles are not necessary for combustion to occur and that carbon can react with metal oxides directly.

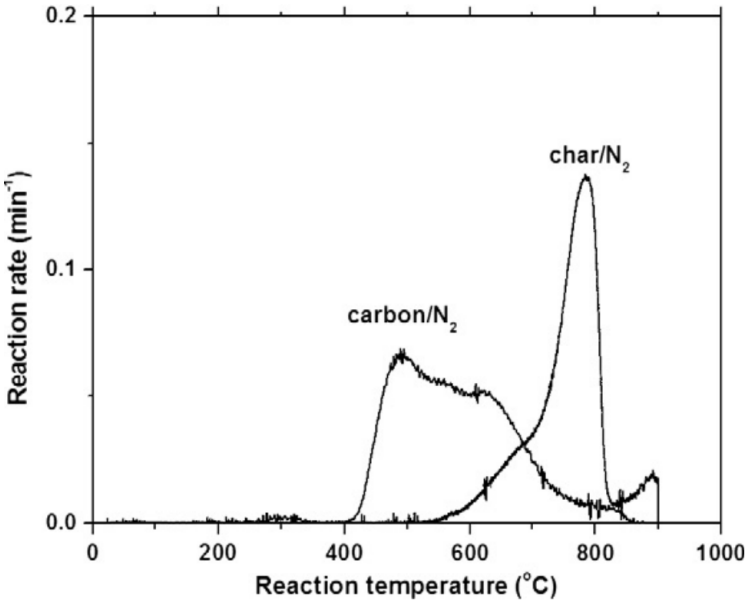


**Figure 3. Reduction reaction performance of CuO with solid fuels** [15]

The two peaks seen in figure 3 for the carbon/$N_2$ line indicate that two combustion reactions exist around 480ºC and 620ºC and x-ray diffraction (XRD) measurements of the carbon-CuO combustion indicated that $Cu_2O$ is created as a reaction intermediate at around

450ºC to 500ºC. Additional measurements of the carbon-CuO reaction using x-ray photoelectron spectroscopy (XPS) showed a decrease in the C/Cu atomic ratio and changes in the Cu oxidation state from $Cu^{2+}$ to $Cu^{+}$ at 440ºC, confirming that the combustion is initiated by the conversion of CuO to $Cu_2O$ and then the reaction proceeds until $Cu_2O$ is converted into Cu metal. TGA data from the combustion of carbon-CuO and carbon-$Cu_2O$ confirmed that the first reaction at 480ºC is due to the reduction of CuO to $Cu_2O$ and the second reaction is the reduction of $Cu_2O$ to metallic Cu at 624ºC, as shown in figure 4.

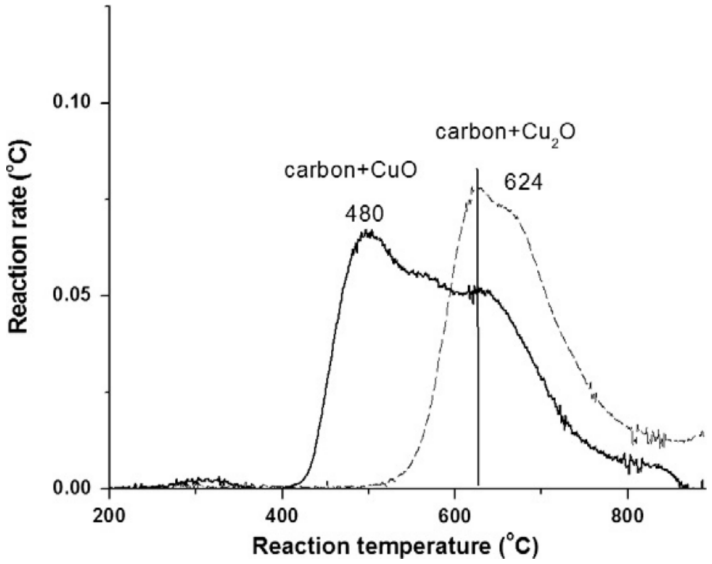


**Figure 4. TGA profile of combustion reaction of carbon with CuO and $Cu_2O$** [15]

Thus, the combustion reaction between carbon fuel and the CuO oxygen carrier consists of a two-step reaction mechanism where CuO is first reduced to $Cu_2O$ at low temperatures, as shown by reaction (5). The $Cu_2O$ intermediate is then fully reduced to metallic Cu when higher temperatures are reached, as shown by reaction (6).

$$4CuO \rightarrow 2Cu_2O + O_2 \quad (5)$$

$$C + 2Cu_2O \rightarrow 4Cu + CO_2 \quad (6)$$

This combustion reaction mechanism involves "fuel induced oxygen release" through solid-solid contact between the carbon fuel and metal oxide. The solid-solid contact is achieved through small particle sizes and surface melting, thus contact points between the C and CuO particles are critical. The combustion reaction can take place at low temperatures of about 500ºC if there is sufficient contact between the two solids, which is a low temperature that cannot be explained through other reaction mechanisms such as fuel gasification or CLOU.

### 1.6 Post-Combustion Oxidation of Copper

Once the copper oxide is reacted with fuel in the combustion reaction, the reduced copper product must undergo re-oxidation in the air reactor in order to continue the CLC loop. In the case of CuO as an oxygen carrier, the CuO is reduced to metallic Cu through combustion with carbon in the fuel reactor, as discussed in section 1.5. The Cu is then passed to the air reactor where the Cu is reduced back into CuO to be recirculated to the fuel reactor. Within the air reactor, the Cu is oxidized with $O_2$ from the air as shown by reaction (7).

$$Cu + \frac{1}{2}O_2 \rightarrow CuO \quad (7)$$

Both the oxidation and reduction reactions for Cu-based oxygen carriers are exothermic, meaning that the recirculation between the air and fuel reactors is not affected by heat balance

[16]. The exothermic reactions also allow for heat extraction from both reactors for energy production.

There is currently little literature with a focus on the oxidation reaction of CuO for the regeneration stage of chemical-looping combustion. García-Labiano et al. [17] studied the reaction kinetics of the reduction and oxidation of CuO supported on alumina created via impregnation. Experiments over varying oxygen concentrations and temperatures revealed that the oxidation of the reduced Cu-based carrier was controlled by chemical kinetics with an activation energy of 15 kJ/mol and a reaction order of 1. Another study conducted by Chuang et al. [18] observed the oxidation of Cu by oxygen over temperatures ranging from 300ºC to 900ºC. The results revealed that the oxidation of Cu can occur directly via Cu to CuO as well as indirectly by forming $Cu_2O$ as an intermediate.

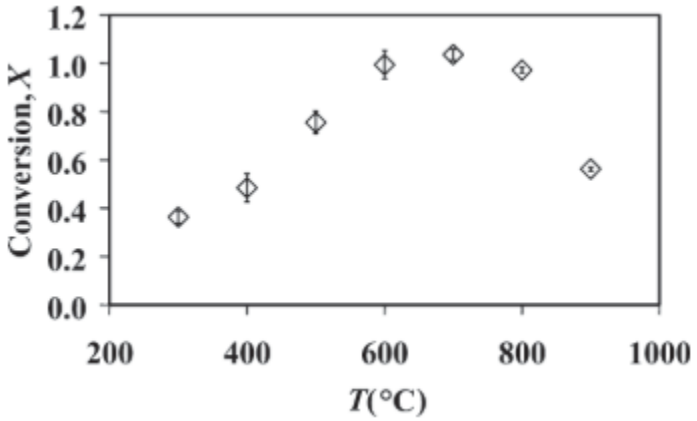


**Figure 5. Final conversion against temperature for oxidation of Cu to CuO at 1.3 vol% $O_2$** [18]

Measurements of the reaction conversion over varying temperatures, shown in figure 5, revealed that below 600ºC, the oxidation reaction was incomplete, with XRD data detecting a mixture of $Cu_2O$, CuO, and some unreacted Cu present within the products. The oxidation shifted to complete formation of CuO at temperatures above 600ºC and was controlled mainly by external

mass transfer. This higher temperature oxidation (600ºC - 900ºC) was found to occur via an indirect reaction mechanism with two consecutive steps, shown by reactions (8) and (9):

$$2Cu + \frac{1}{2}O_2 \rightarrow Cu_2O, \quad \Delta H^0_{1073\,K} = -167.3\ kJ/mol \tag{8}$$

$$Cu_2O + \frac{1}{2}O_2 \rightarrow 2CuO, \quad \Delta H^0_{1073\,K} = -131.5\ kJ/mol \tag{9}$$

Also shown in figure 5, the conversion drops again at 900ºC. This is because at these temperatures, $Cu_2O$ is thermodynamically favored and the fully oxidized carrier is decomposed to $Cu_2O$ and $O_2$. Thus, similar to the two-step reduction reaction, the oxidation of Cu involves an intermediate of $Cu_2O$ and temperatures between 600ºC and 900ºC are optimal in order for Cu to completely oxidize to CuO.

### 1.7 Research Goal and Objectives

While chemical-looping combustion has been researched for many years, much remains unknown about certain CLC methods and processes. In particular, CLC through solid-solid combustion of carbon fuel with a metal oxide shows promise in creating an easier and cheaper CLC mechanism, however there is little research behind this topic. Also, all of the aforementioned studies utilized an externally heated reactor to examine the metal oxide and fuel combustion. However, if a hot-spot is produced in a packed mixture of copper oxide and carbon fuel, the reaction may react rapidly and become self-propagating via a combination of solid-solid interactions and oxygen uncoupling. The goal of this thesis is to test this self-propagating reaction in order to better understand the combustion reaction of solid carbon fuel with copper

oxide to evaluate it as a feasible approach to CLC. This goal will be accomplished through the following research objectives:

- Model the combustion reaction using a mixture of solid carbon and copper oxide packed into a quartz tube with a furnace supplying an initial temperature. The combustion will be initiated by a $CO_2$ laser and recorded on a high-speed camera.
- Analyze the effect of various experimental parameters on the combustion reaction and flame propagation. Parameters will include various preheat temperatures and particle sizes.
- Observe differences between copper oxide oxidation states by testing both CuO and $Cu_2O$ as metal oxides for the combustion reaction.

These objectives will lead to a better understanding of the solid fuel reactions in chemical-looping combustion in order to progress the technology towards industry ready where it can begin to improve energy production by reducing harmful carbon dioxide release.

# Chapter 2

# Experimental Methods

## 2.1 Copper Oxide Sample Preparation

As discussed in chapter 1, copper oxide is a leading candidate for many CLC applications including CLOU and fuel induced oxygen release methods. For this reason, copper oxide was chosen as the focal metal oxide for this study. Multiple variants of copper oxide powders were observed including copper(II) oxide (CuO) with micrometer-sized particles and nanometer-sized particles as well as copper(I) oxide ($Cu_2O$) micrometer-sized particles. Table 1 shows the molecular properties of all metal oxides used in this experiment. All copper oxide powders were manufactured and purchased from Sigma-Aldrich chemicals company.

**Table 1. Metal Oxide Properties**

| Metal Oxide | Empirical Formula | Particle Size | Molecular Wt. (g/mol) | Density ($g/cm^3$) |
|---|---|---|---|---|
| **Copper(II) Oxide nanoparticles** | CuO | <50nm | 79.55 | 6.31 |
| **Copper(II) Oxide microparticles** | CuO | <10µm | 79.55 | 6.31 |
| **Copper(I) Oxide microparticles** | $Cu_2O$ | <7µm | 143.09 | 6.0 |

The fuel utilized for the combustion reaction was Monarch 120 carbon black powder from Cabot with a molecular weight of 12 g/mol, a particle size of 60 nm, and a particle density of 1.8 $g/cm^3$. Stoichiometry for CuO was determined through equation (10) which yields a fuel to oxidizer ratio (F/O) of $7.54x10^{-2}$ on mass basis. Similarly, the stoichiometry for the $Cu_2O$

reaction was determined through equation (11), yielding a fuel/oxidizer ratio of $4.19 \times 10^{-2}$ on mass basis.

$$2CuO + C(s) \rightarrow 2Cu(s) + CO_2 \quad (10)$$

$$2Cu_2O + C(s) \rightarrow 4Cu(s) + CO_2 \quad (11)$$

The masses of carbon fuel and copper oxide powders to be mixed were calculated through equations (12) and (13) respectively using the desired equivalence ratio ($\phi$) and batch mass ($M_{total}$) for the experiment.

$$M_{fuel} = \frac{M_{total}}{1 + \frac{1}{F/O \cdot \phi}} \quad (12)$$

$$M_{oxidizer} = \frac{M_{fuel}}{F/O \cdot \phi} \quad (13)$$

Batches were made for a total mass of 2.15g in order to yield two samples of approximately 1g each with an extra 0.15g to account for losses occurred while transporting the mixture between vials and while loading into testing tubes. All tests in this research were conducted at a stoichiometric equivalence ratio of one, meaning that all fuel and oxidizer particles should be converted during the combustion. An equivalence ratio of more than one would indicate that there is more fuel than oxidizer, which is known as fuel rich, while an equivalence ratio of less than one would indicate there is an abundance of oxidizer, known as a fuel lean reaction.

The copper(I) oxide ($Cu_2O$) powder particles purchased by Sigma-Aldrich were stored with a stabilizer coating of 0.5% stearic acid in order to prevent clumping during shipping and storage. The stabilizer would interfere with the combustion reaction being tested and additional procedures were required to remove the stearic acid coating from the $Cu_2O$ particles. Stearic acid is soluble in hexane at 0.5g/100g at 20ºC thus, prior to mixing with the carbon 120 fuel the

calculated mass of $Cu_2O$ for one batch was washed with approximately 5mL of hexane. The $Cu_2O$ – hexane mixture was shaken and left untouched for at least 30 minutes to allow the stearic acid to dissolve and the $Cu_2O$ particles to settle. After the 30 minutes, the stearic acid was decanted off of the top of the mixture using a pipet, leaving behind the washed $Cu_2O$ particles. This process was repeated again to assure all of the stearic acid stabilizer was removed and the washed $Cu_2O$ powder then proceeded to the fuel mixing process identical to the CuO powders.

The calculated masses of copper oxide and carbon 120 fuel were combined in a glass vial with approximately 8-10 mL of hexane to suspend the particles. The vial was then placed under a sonicating horn and ultrasonically mixed for 0.5s on and 0.5s off for 1 minute. After sonicating, the sample was assumed adequately mixed and was spread out on a stainless-steel pan heated to approximately 40ºC to evaporate the hexane. The dried mixture was passed through a sieve to eliminate clumping and bottled until sample testing. Each mixture batch yielded approximately 2.15g of the CuO/C mixture, which was enough for two 1g samples for the experiment with an excess to account for any transportation losses. During sample testing, 1g of the created batch mixture was massed out and funneled into a 0.8cm inner diameter quartz tube with a graphite plug on one side. The mixture was then packed to a specified length based off of the desired density of the packed powder sample.

## 2.2 Combustion Experimental Setup

The combustion experimental setup consisted of the quartz tube containing the packed copper oxide – carbon 120 fuel sample placed inside of a furnace to provide an initial preheat temperature ranging from 100ºC to 450ºC. A temperature controller with a thermocouple placed inside of the furnace directly by the sample was used to regulate the furnace internal temperature. Once the sample was properly aligned, the furnace was closed and heated to the desired preheat temperature. The sample was allowed to soak at the desired temperature for approximately 10 minutes to ensure uniform heating. A 70W Synrad $CO_2$ laser was used to ignite a hotspot in the mixture from the end opposite of the graphite plug. Once the sample was ignited by the $CO_2$ laser, the resulting flame propagation was captured on a micro Nikkor camera with a 105mm lens using StreamPix 6 recording software. The camera settings used can be seen in table 2.

**Table 2. 105 mm Nikkor and Streampix 6 camera settings.**

| Frame Rate | F-Stop | Pixel Clock | Exposure |
|---|---|---|---|
| 59.936 fps | 11 | 86 MHz | 9.9836 ms |

Experiments where the combustion reaction temperature was monitored utilized a k-type thermocouple placed in the center of the sample. A schematic of the experimental setup can be seen in figure 6.

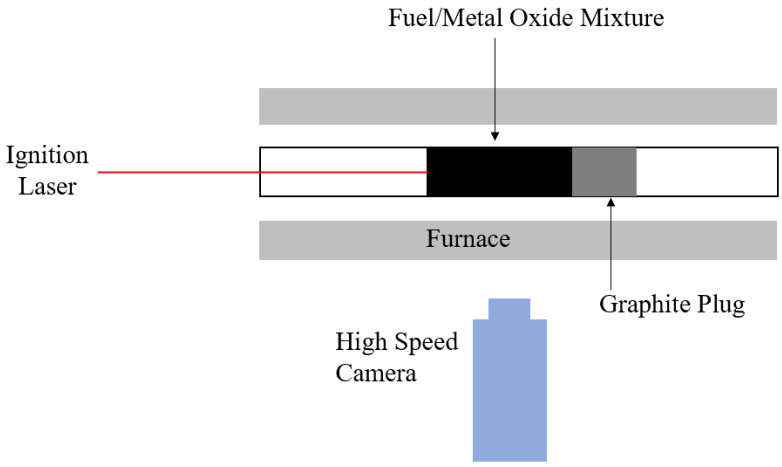


**Figure 6. Schematic of combustion reaction experimental setup**

Images of the experimental setup and equipment as well as images of the raw chemical materials used in this research can be found in Appendix A. The experimental standard operating proceedures that were followed to conduct testing can be found in Appendix B.

# Chapter 3

# Results and Discussion

## 3.1 Influence of Preheat Temperature

Once a hot spot was ignited with the $CO_2$ laser, the nano-particle CuO/C mixture became self-propagating with a luminous flame front travelling down the tube. This flame front was captured on the high-speed camera and processed using ImageJ video software where the distance the flame travelled between frames could be extracted. The nano-particle CuO/C mixture was tested at preheat temperatures ranging from 100ºC to 450ºC. Figure 7 shows a sequence of frames from the combustion of nano-particle CuO and carbon 120 powder preheated to 400ºC.

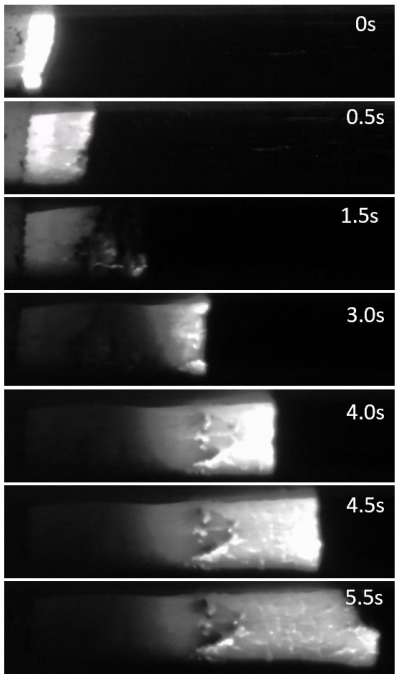


**Figure 7. Image frames of nano-CuO/C combustion propagation preheated to 400ºC**

Figure 7 demonstrates that once a hot-spot was induced with the laser at 0 seconds, the reaction became self-propagating towards the end of the tube until it reached the graphite plug. In many samples the flame had some inconsistencies, as with figure 7 around 1.5s where the flame is only propagating along the bottom of the tube, however it returns to full propagation until completion. These inconsistencies could be due to a variety of factors such as non-uniform packing density, heating, or mixing caused by limitations in equipment and human error.

By capturing the propagation frame-by-frame and knowing the frame rate of the camera, the time elapsed at each frame could be calculated as frame number divided by frame rate (FPS). The flame propagation distance in millimeters was then plotted against the time elapsed in seconds and the flame propagation speed in mm/s was found using the slope of a linear fit line of the distance versus time plot. Figure 8 shows the distance versus time plot of the same 400ºC preheated sample captured in figure 7.

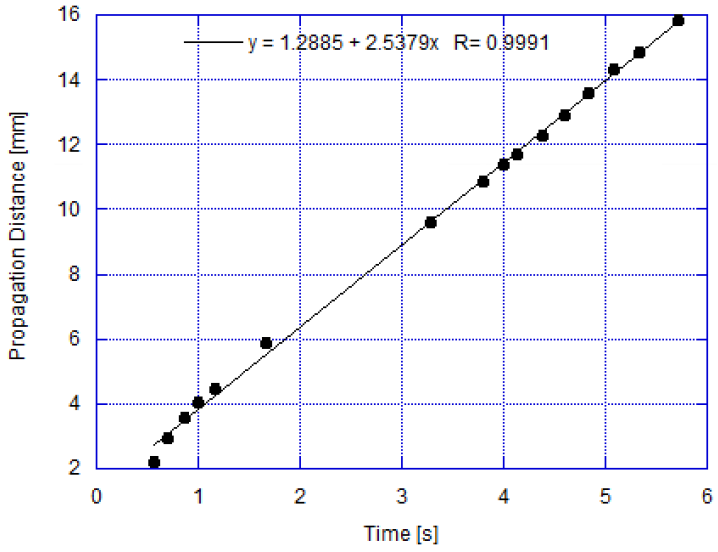


**Figure 8. Distance vs. time plot of nano-CuO/C preheated to 400ºC**

After the laser ignition, the propagation became very linear with a constant speed throughout the sample, which was the case for the majority of samples. However, inconsistent propagation

speeds were observed in some of the samples, where the reaction would appear to quench partially through the sample and then begin propagation again at a higher speed. This again could possibly be due to errors in preparation that cause a non-uniform sample or be caused by varying reaction mechanisms, which will be discussed.

The varying preheating temperatures of the samples showed an influence on the intensity and flame shape of the combustion propagation. Samples preheated to temperatures under approximately 250ºC often propagated slower with a less luminous flame front compared to samples preheated above 250ºC. The lower temperature reactions also had a less coherent flame front, propagating circumferentially in small spots of the tube rather than linearly across the entire diameter of the tube, as with the higher temperature reactions. Figure 9 shows a comparison of a sample ignited at 400ºC against a sample ignited at 150ºC.

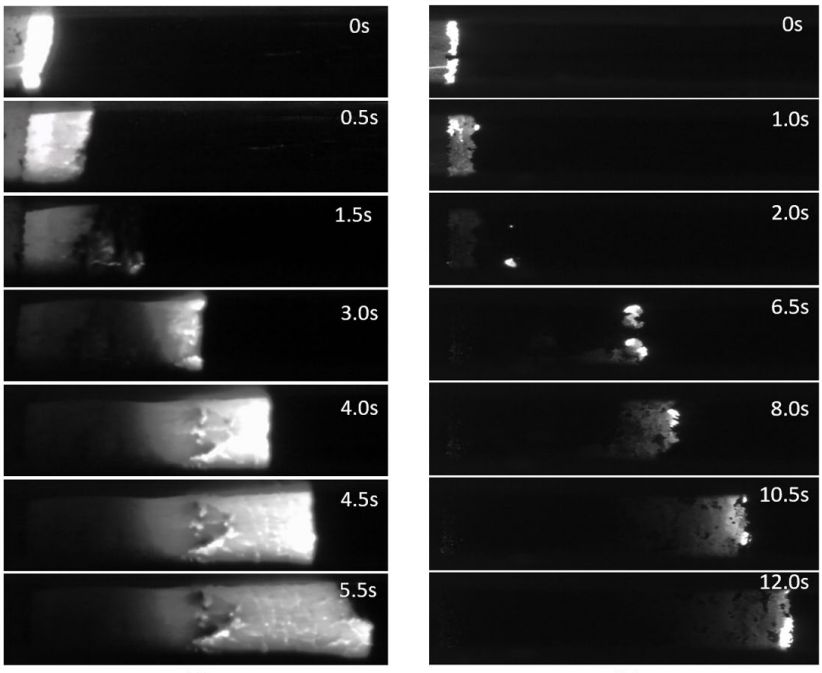


**Figure 9. Nano-CuO/C mixture reaction preheated to 400ºC (a) and preheated to 150ºC (b)**

The lower temperature sample in (b) propagated via small pockets of combustion while the higher temperature sample in (a) had a luminous and coherent flame front. This propagation difference was a common trend, as higher preheat temperatures resulted in coherent flame fronts spanning nearly the entire diameter of the tube, while lower temperatures propagated through smaller channels and pockets, often leaving portions of the sample unreacted.

A possible explanation for this difference is that the changing preheating temperatures caused a variation in the primary reaction mechanism. As discussed in chapter 1, oxygen uncoupling requires reaction temperatures typically above 800ºC, therefore the samples preheated to lower temperatures may not have reached a high enough reaction temperature to create oxygen uncoupling of the copper oxide and thus proceeded only via a solid-solid reaction mechanism. Contact points between the fuel and metal oxide particles are critical for the solid-solid reaction to occur, therefore the reaction only occurred where there was significant contact between the fuel and oxide resulting in the observed smaller pockets of combustion rather than a coherent flame front. The higher preheated reactions on the other hand may have reached a high enough reaction temperature to induce gaseous oxygen release from the copper oxide. The oxygen release allowed the combustion to proceed via a combination of solid-solid contact reactions as well as fuel reactions with gaseous oxygen. The oxygen uncoupling reaction utilizes gaseous oxygen disbursed throughout the tube rather than contact points and therefore created a more coherent flame front throughout the tube diameter.

Preheating temperature also showed an influence on the propagation speed of the combustion reaction. Figure 10 shows a plot of the average propagation flame speed across the various preheat temperatures.

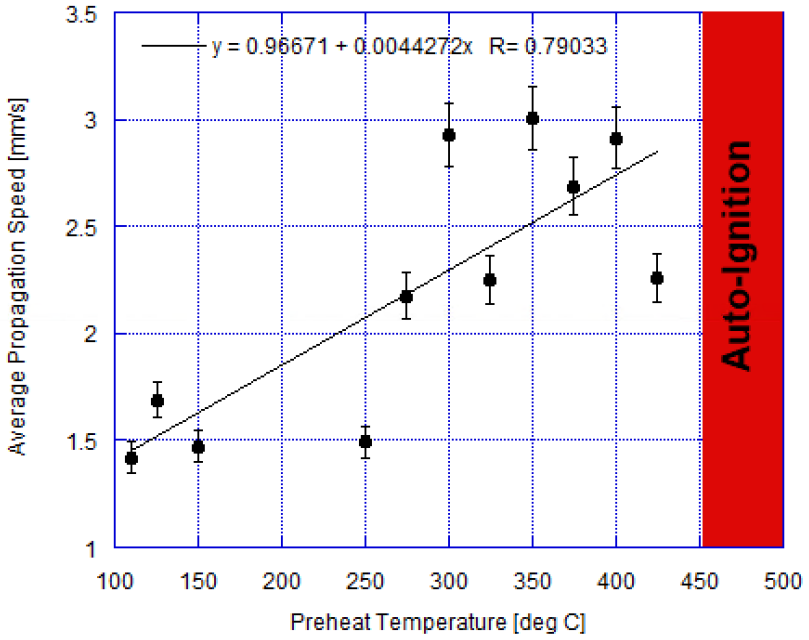


**Figure 10. Propagation speed vs. preheat temperature of nano-particle CuO/C combustion**

Figure 10 reveals a linear trend of higher reaction propagation speeds with increasing preheat temperatures. As previously mentioned, samples may have been limited to solid-solid reaction mechanisms without oxygen uncoupling assisting the reaction at lower preheat temperatures. Previous studies also indicate that the solid-solid reaction occurs at slower rates than other mechanisms, specifically CLOU, which may have been a contributor to the slower propagation speeds at lower temperatures. The nano-CuO/C mixture was also observed to auto-ignite without the use of the ignition laser at temperatures above 450ºC, indicating this is the temperature required to activate the CuO/C combustion reaction.

### 3.2 Influence of Particle Size

Two different CuO particle sizes were tested in order to observe the influence of particle sizes on the combustion reaction. Reactions of carbon 120 fuel with microparticle CuO powder with a particle size of <10µm were compared to reactions using nanoparticle CuO powder with a particle size of <50nm. The particle size has a great influence on the bulk density of the sample as well as the number of contact points between the fuel and copper oxide. The smaller nanoparticles have a greater surface area among them and can create more contact points with the fuel. The increased surface area also causes increased friction between particles leading to a fluffier powder with a lower bulk density in the nanoparticles compared to the more compact samples created with the microparticles. When loading the 1g samples into the quartz tube, the larger particle micro-CuO/C mixture had an unpacked length of about 1.5cm, where the nano-CuO/C mixture had an unpacked length of about 2.2cm. Both samples were packed an additional 2mm to create a packed sample. Approximating the metal oxide particles to be spheres, the max volume fraction for random packing is known to be approximately 64%. Neglecting the mass of air in the voids, the theoretical maximum bulk density of the sample is approximately 64% of the particle density. The micro-CuO/C mixture was packed to 1.3cm yielding a bulk density of 1.53 $g/cm^3$, which is approximately 38% of the theoretical maximum density for CuO. The nano-CuO/C mixture was packed to 2.0cm, yielding a bulk density of 0.995 $g/cm^3$, which is approximately 25% of the theoretical maximum.

Both particle sizes were tested across the same preheat temperature range of 100ºC to 450ºC. From visual observation of the sample propagation videos, the microparticles propagated with a less luminous and less coherent flame front than the nanoparticles. Figure 11 shows a

comparison of the nano-CuO/C combustion (a) compared to the micro-CuO/C combustion (b) both at a preheat temperature of 400ºC.

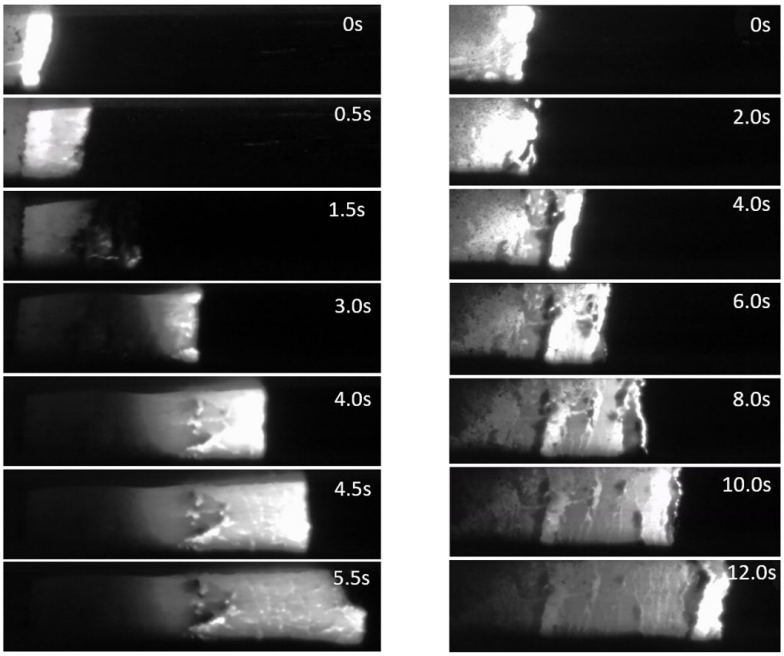


**Figure 11. Nano-CuO/C combustion (a) and micro-CuO/C combustion (b) both preheated to 400ºC**

The nanoparticle combustion flame appeared more luminous than the microparticle reaction. The nanoparticle reaction also had a more coherent and consistent flame front, as the microparticle combustion was more sporadic and often propagated circumferentially around the tube rather than directly forward. The combustion flame of the microparticle reaction also propagated much slower than the nanoparticle combustion flame, taking approximately twice as long until full propagation. For these two samples, the average flame propagation speed for the nanoparticle reaction was 2.54 mm/s while the average propagation speed of the microparticle reaction was 0.721 mm/s. This significantly slower propagation speed was a typical trend with the increased particle sizes. As shown by figure 12, the microparticle reaction was consistently slower than the nanoparticle reaction across all temperatures.

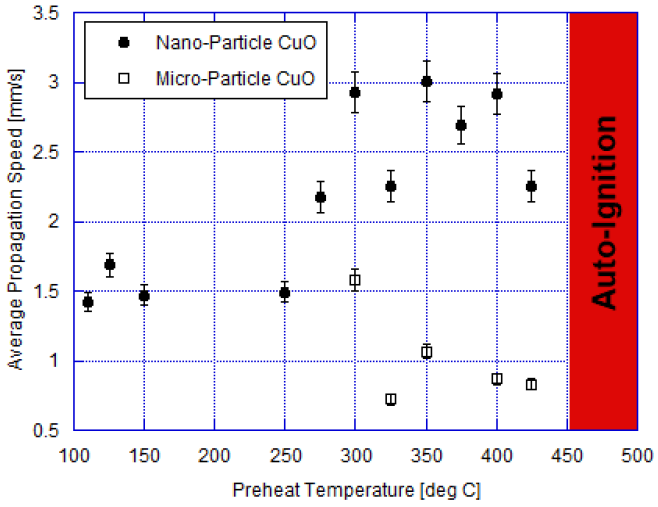


**Figure 12. Average propagation speed of micro-particle and nano-particle CuO/C**

The microparticle mixture had larger air voids between the particles creating fewer solid contact points between the fuel and copper oxide due to the increased particle volume and decreased available surface area. Fewer solid contact points significantly reduced the likelihood of a solid-solid reaction because contact points are critical for this mechanism. The microparticle reaction may have proceeded through some oxygen uncoupling, but with less assistance from the solid-solid reaction than with the nanoparticles. The solid-solid reaction of the nano-CuO/C samples at higher preheat temperatures could have worked to increase the reaction temperature enough to induce a significant amount of oxygen release from unreacted CuO and create combustion via CLOU mechanisms. Thus, it is possible that the reaction mechanisms within the nanoparticle samples worked in tandem to create faster propagation speeds. The micro-CuO/C samples had less contact points for the solid-solid reaction to proceed, which reduced the amount of heat produced through combustion and caused less oxygen to be released by CuO, limiting the impact of CLOU mechanisms on the propagation. The microparticle reactions also failed to propagate at temperatures below 300ºC whereas the nanoparticle reactions propagated as low as 100ºC. As previously mentioned, CLOU based reactions are likely limited at lower preheat

temperatures and the decreased contact points in the microparticles also reduced the impact of solid-solid reactions thus, the combustion did not occur with microparticles at low temperatures.

The auto-ignition temperature of the micro-CuO/C reaction was consistent with the auto-ignition temperature of the nano-CuO/C samples at around 450ºC, indicating that particle size does not influence the auto-ignition point. However, during auto-ignition of the nano-CuO/C mixture, the sample showed a bright ignition throughout, whereas the micro-CuO/C auto-ignition did not give off any significant light and simply propelled itself towards the opening of the tube. Figure 13 shows images of the auto-ignited samples of both particle sizes.

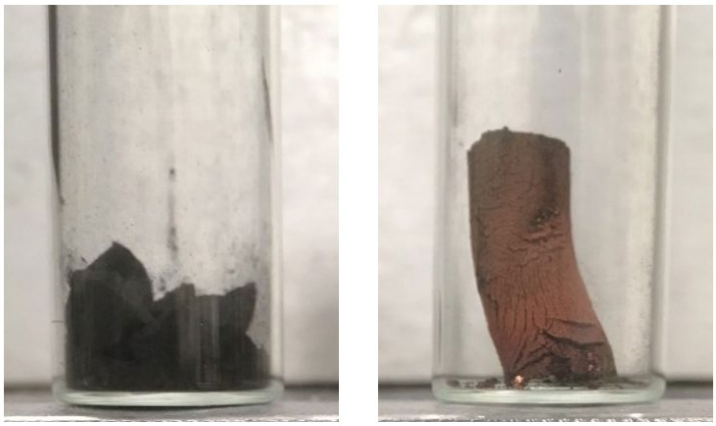


**Figure 13. Auto-ignited samples of microparticle CuO/C (a) and nanoparticle CuO/C (b)**

The nanoparticle sample in (b) turned the originally black sample to a red-orange color and clearly underwent a combustion reaction. However, the microparticle sample in (a) remained the black color of the original CuO/C mixture and does not appear to have underwent a significant chemical reaction. Gaseous buildup may have caused the ejection of the micro-CuO/C mixture during auto-ignition without enough solid-solid interaction to induce combustion.

From these experiments, the nanoparticle CuO was more reactive across a wider range of temperatures compared with the microparticle CuO. The nanoparticles also created higher

propagation speeds. It is proposed that the differences in propagation rates and reactivities was due to the decrease in contact points between the oxide and fuel particles, which have been shown to be critical for solid fuel CLC.

### 3.3 Influence of Oxidation State

As discussed in chapter 1, the reduction reaction for CuO occurs in two steps: first the CuO is reduced to $Cu_2O$, shown in equation (14), and then reduced to Cu as shown by equation (15). The first reduction to form $Cu_2O$ can occur at a lower temperature (around 480ºC) and the second step requires a higher temperature (around 620ºC) to form Cu. From this reaction mechanism, it is shown that the CLC reaction of CuO can produce intermediate products of $Cu_2O$ if the reaction does not reach a high enough temperature to fully reduce to solid copper.

$$4CuO \rightarrow 2Cu_2O + O_2 \quad (14)$$

$$C + 2Cu_2O \rightarrow 4Cu + CO_2 \quad (15)$$

Visual inspection of the products from the combusted nanoparticle CuO/C samples revealed the formation of metallic pockets near the center of the sample where the laser ignition had occurred, shown in figure 14 (a). This area is assumed to be the hottest region of reaction and thus it is likely that the metallic areas are solid copper formations that had been melted together. Outside of the metallic areas, the reaction turned the originally black CuO/C mixture to a dark red/brown color, shown through (b) in figure 14.

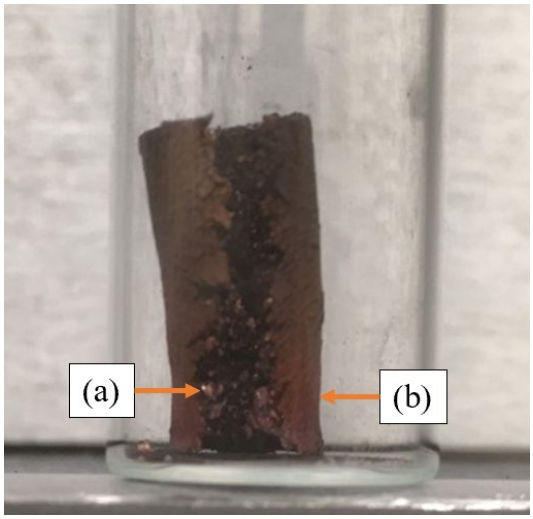


**Figure 14. Image of the post combustion products from the CuO/C self-propagation reaction**

Unreacted $Cu_2O$ is also known to have a similar dark red/brown coloring, which may indicate that the CuO combustion reaction produced $Cu_2O$ throughout the majority of the sample. The outer edges farther from the ignition point may not have reached a high enough reaction temperature to form fully reduced copper. Therefore, it is likely that the self-propagating reaction that occurred within the CuO/C mixture did not fully reduce to solid copper, but rather to a reaction intermediate of $Cu_2O$ with small formations of Cu.

To further explore this theory, copper(I) oxide ($Cu_2O$) was used as an oxidizer in place of the copper(II) oxide (CuO) to test the effect of using the reaction intermediate at the start of combustion. The $Cu_2O$ samples were mixed at the same equivalence ratio of one and with the same carbon 120 fuel as the CuO samples. The combustion experiments revealed that the $Cu_2O$ samples did not become self-propagating across the same temperature range as the CuO samples. No propagation was observed with $Cu_2O$ until a preheat temperature of approximately 425ºC. Even preheat temperatures above 425ºC did not create significant propagation after ignition, as the $Cu_2O$/C reaction propagated slowly and quenched roughly a quarter way through the sample. The $Cu_2O$ sample was also observed to auto-ignite at approximately 625ºC, where the sample

ignited without the laser and quickly ejected towards the front of the tube. The $Cu_2O$ auto-ignition temperature of 625ºC was much higher than the auto-ignition temperature of 450ºC observed with the CuO/C mixtures. The high temperatures required for the $Cu_2O$ reaction reinforce the theory that the combustion reactions with CuO stopped at the $Cu_2O$ reaction intermediate rather than fully reducing to Cu because the CuO reaction did not reach a high enough temperature to proceed to the reduction of $Cu_2O$. These observations also coincide with findings in other studies discussed in chapter 1 that report the $Cu_2O$ to Cu reduction reaction occurring at much higher temperatures than the CuO to $Cu_2O$ reaction. $Cu_2O$ has also been shown through other studies to require a higher temperature for gaseous oxygen release through oxygen uncoupling. This lack of gaseous oxygen released along with fewer contact points caused by the micrometer-sized $Cu_2O$ particles could be contributors to the lack of self-propagation observed in the $Cu_2O$ samples.

The auto-ignited samples of $Cu_2O$/C were the only samples believed to have fully combusted, as the reactions at preheat temperatures lower than the auto-ignition point of 625ºC were quickly quenched. The auto-ignited samples were observed to change color from the unreacted dark red/brown coloring to a lighter, red/orange coloring. Figure 15 shows images of the auto-ignited $Cu_2O$/C mixture (a) compared with a $Cu_2O$/C sample heated to a lower temperature that quickly quenched upon ignition (b).

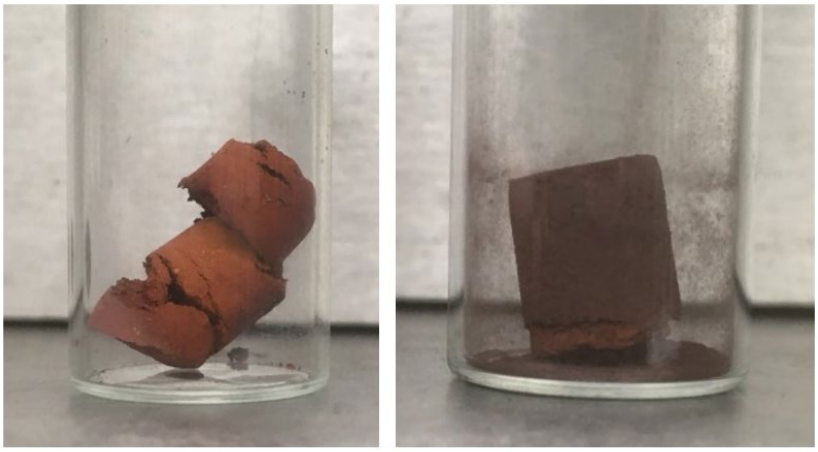

(a) (b)

**Figure 15. Products of $Cu_2O$/C reaction when auto-ignited (a) and when quenched (b)**

The color change is a strong indication that a chemical reaction occurred in the auto-ignited sample (a), which was likely the reduction of $Cu_2O$ to Cu and the consumption of the carbon fuel from the combustion reaction. The quenched reaction in figure 15 (b) did not change in color and it was assumed to be unreacted through the majority of the sample.

# Chapter 4

## Conclusion and Future Work

Chemical-looping combustion is a promising technology for reducing carbon emissions during fossil fuel energy production. Many leading CLC methods currently in practice were discussed in chapter 1 of this thesis, however all previous research discussed utilized an externally heated reactor to carry out the combustion reaction. This thesis investigated the possibility of a self-propagating reaction between a mixture of copper oxide and carbon 120 solid fuel initiated by a laser hot-spot. Multiple experimental parameters were varied including preheat temperature, metal oxide particle size, and oxidation state of the metal oxide in order to evaluate their influence on the combustion reaction.

Self-propagating CLC reactions with mixtures of nanoparticle copper(II) oxide powder and carbon 120 fuel were observed at preheating temperatures as low as 110ºC. Increasing the preheat temperature created a more luminous and coherent flame front that traveled at faster propagation speeds. It was proposed that the lower temperature reactions proceeded primarily through a solid-solid reaction mechanism and the increase in flame coherence and propagation speeds at higher temperatures was due to the introduction of oxygen uncoupling reaction mechanisms to assist with the combustion propagation. The use of larger sized microparticle copper(II) oxide powders revealed significantly slower propagation speeds and less coherent flame fronts when compared to the nanoparticle combustions. Since contact points between the metal oxide and fuel are critical for solid-solid reactions, it was suggested that the difference in propagation speed and flame intensity was due to the reduction in contact points created by

larger particle sizes. Visual observations of the CuO/C combustion reaction products indicated that the copper(II) oxide may have been mostly reduced to copper(I) oxide during the self-propagating reaction, with small deposits of solid copper near the ignition point. Lastly, the propagation experiment was conducted using copper(I) oxide as a metal oxide, which revealed a much higher auto-ignition temperature as well as shorter and less frequent self-propagating reactions. A summary of the important metrics found in this study can be seen in table 3.

**Table 3. Summary of important metrics for different oxidizers**

| Metal Oxide | Max Speed | Propagation Range | Auto-Ignition |
|---|---|---|---|
| **Nano-CuO** | 6.53 mm/s | 110ºC - 450ºC | 450ºC |
| **Micro-CuO** | 1.74 mm/s | 300ºC - 450ºC | 450ºC |
| **Micro-$Cu_2O$** | 1.18 mm/s* | 400ºC - 625ºC* | 625ºC |

* $Cu_2O$ propagations did not travel entire sample length

Future work will focus on confirming the proposed reaction mechanisms discussed in this thesis. The products formed during all reactions discussed in this research were preserved for analysis. These products should be further analyzed in order to identify the molecular content and confirm or reject the idea that the CuO reactions reduced primarily to $Cu_2O$ and that the $Cu_2O$ auto-ignited reactions formed Cu. Also, various sample densities, packing methods, and mixing methods should be explored since contact points have been identified as a critical factor for the solid-solid reaction. Lastly, the post-combustion oxidation reaction was not investigated as a part of this thesis and is a topic that is not widely studied in literature. The oxidation reaction of copper oxide is also exothermic and may exhibit a self-propagation similar to the combustion reactions observed in this thesis. The oxidation reaction should also be explored in future work in order to further progress the understanding of chemical-looping combustion methods.

# Appendix A

## Images of Experimental Materials, Equipment, and Setup

(a) (b) (c)

Figure 16-A. Images of raw CuO (a), Carbon 120 (b), and $Cu_2O$ (c) particles

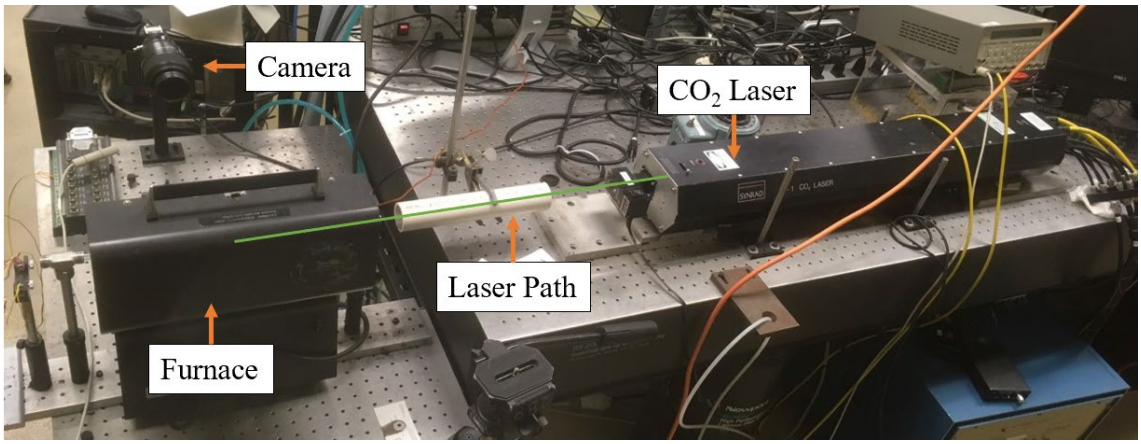


Figure 17-A. Image of combustion reaction experimental setup

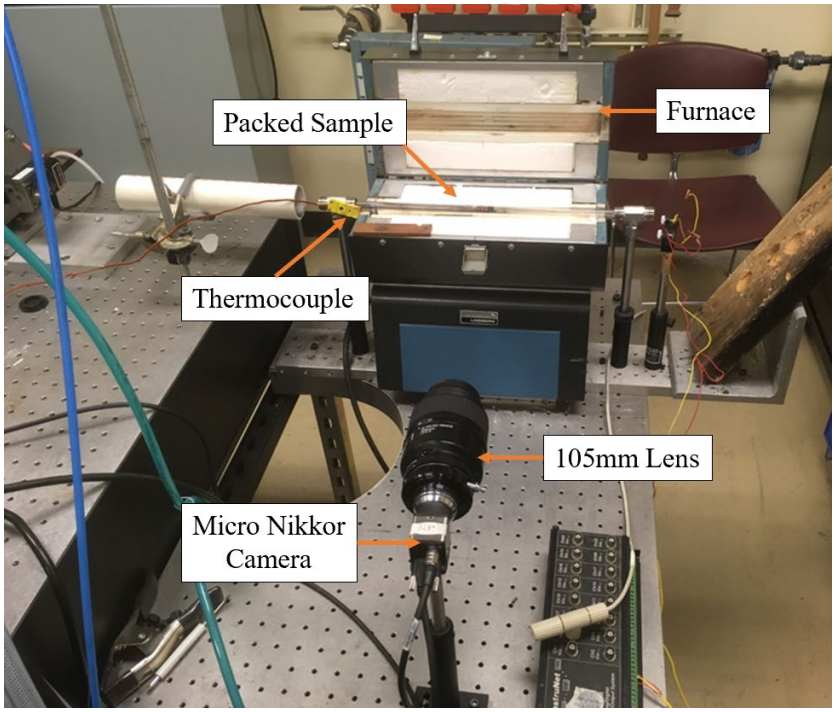


Figure 18-A. Image of camera and open preheating furnace with sample

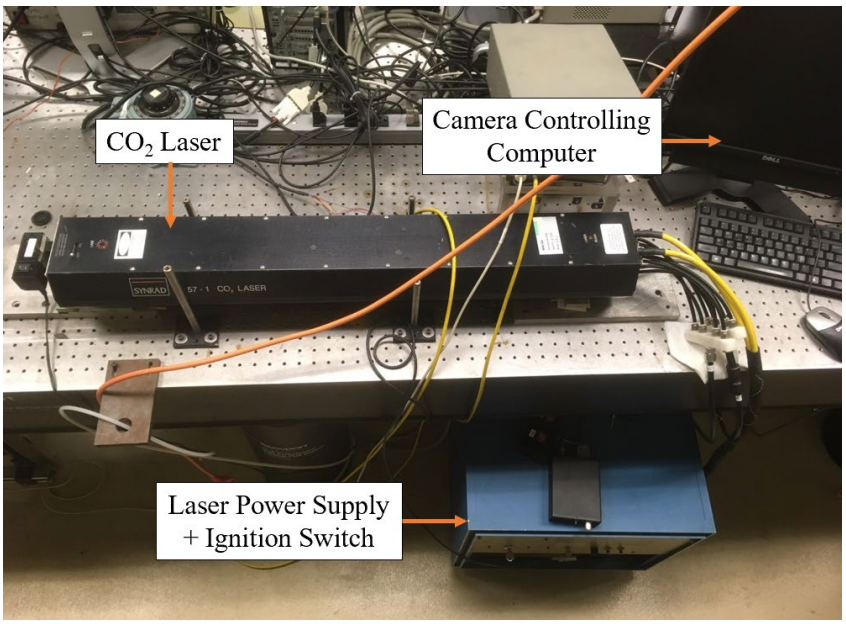


Figure 19-A. Image of sample ignition laser and camera controlling computer

# Appendix B

## Experiment Standard Operating Procedures

### Carbon and Copper(II) Oxide Mixing Procedures

1. Put on the necessary PPE (Nitrile gloves, Respirator).
2. Materials: 20mL scintillation vial, particles being mixed, hexane, pipet, 200W hot plate, steel pan, aluminum foil, weighing paper, thermocouple, plastic collector, quartz tubing, two plungers, graphite plug, scale, sonicator, fume hood, sieve, and brush.
    a. Scales should be cleaned and calibrated every 3 weeks.
    b. Sieve and brush should be cleaned before using different oxidizers/fuels.
3. Using weighing paper and a scale, measure out the desired amount of oxidizer(s), then pour into the vial.
4. Using weighing paper and a scale, measure out the desired amount of fuel(s), then pour into the same vial containing the oxidizer(s).
5. Pipet hexane into the vial containing the mixture until the hexane is:
    a. A little above half full - 1.1g batch
    b. ¾ full - >2.15g batch.
6. Apply a small piece of aluminum foil on vial opening and punch a small hole to allow the sonicator tip to enter.
7. Situate the sonicator tip in the center of vial, making sure that the sonicator tip does not make contact with any glass surface.
8. Sonicate the vial for 30 s for 0.5 s on, 0.5 s off, 46% duty-cycle at 450W (1 min total). Note: It is normal for the vial to be warm post sonication.
    a. Sonication of a batch size >2.15g may agglomerate and can be identified by a high pitch sound, which should not to be confused with the sonicator tip touching the glass. In this situation, sonicate the batch for 30s, 0.2 s on, 0.8 s off, 40% duty cycle at 450W.
9. Wait for 1-2 mins until the vial is at room temperature.
10. Repeat step 9. Note: This step may be repeated more times depending on how mixed the material is by visual inspection.
11. Place the hot plate under the fume hood.
12. Place steel pan on the hot plate.
13. Turn on the hot plate and wait until it is heated to 40°C using the thermocouple.
14. Turn on the fume hood.
15. Pour the vial's contents into the steel pan. Make sure that most, if not all, the vial's contents is poured out. This step may take a couple attempts that require pipeting hexane onto the inside walls of the vial to remove clumping, then pouring again.
16. Wait for 10-20 min.
17. Using the brush, remove the mixture and pour the powder onto the sieve.

18. Using the brush, sieve the mixture into the plastic collector below it.
    a. Use a different plastic collector for different equivalence ratios/mixes.
19. Pour the sieved mixture out of the plastic collector and into a new vial.
20. Finally when ready to create a sample, pour and measure the desired amount of the mixture using a scale.
21. On one end insert the graphite plug while holding its position with a plunger.
    a. If using a thermocouple, make sure it is protruting from the graphite plug into the sample.
22. Next pour the measured amount of the mixture into the quartz tubing opposite to the plunger/graphite end.
23. Compress the sample using another plunger to the desired sample length.
    a. If using a thermocouple, pack lightly/slowly.

**Copper(I) Oxide Washing Procedures**

1. Mass out approximately 5 grams of copper(I) oxide and place in a glass vial.
2. Add approximately 8 ml of hexane to the copper(I) oxide vial.
3. Shake vigorously or sonicate to mix the metal oxide throughout the hexane.
4. Let the vial sit undisturbed for at least 30 minutes to allow the copper(I) oxide particles to settle to the bottom of the hexane.
5. After 30 minutes, carefully use a pipet to decant the hexane off of the top.
6. Add 8 more mL of hexane and repeat steps 2-5 to do a secondary wash.
7. After the second wash, place the wet copper(I) oxide on a heating pan to evaporate off any remaining hexane.
8. Once dried, brush the copper(I) oxide through a sieve to eliminate clumping.
9. Store in a glass vial until it is to be mixed following the carbon and copper oxide mixing procedures.

**$CO_2$ Laser Operation**

**I. PERSONNEL**

1. Experiments operated within a test cell or other confined space require that a minimum of 2 personnel be present to permit operation. Both personnel must be trained, and have previously demonstrated their training by participating in a firing evolution, while being evaluated by qualified personnel.
2. Experiments operated external of a test cell or other confined space require only one person be present to permit operation, provided the operator has completed all lab safety training requirements and has been properly trained to conduct the experiments.
3. Personnel will have completed the EHS laser safety training as well as obtained direct training on the specific laser to be used from a qualified operator and demonstrated their ability to setup and operate the laser safely.

**II. PERSONAL PROTECTIVE EQUIPMENT (PPE)**

1. The minimum required personnel protective equipment (PPE) shall be worn at all times while the laser power supply is turned ON. Additional necessary PPE may be required depending on materials being used and experiments being conducted. These PPE include the following:
    - $CO_2$ laser goggles (required when laser power supply is turned ON).
    - Face Shield or safety glasses.
    - Neoprene (or Neoprene equivalent) chemically resistant gloves.
    - Lab jacket (if necessary).

## III. SPECIFIC LASER INFORMATION

1. The Synrad CO2 laser is a class IV continuous wave laser. The power output is variable from 0 to approximately 115W. The beam wavelength is 10.6μm.

## IV. PRE-STARTUP REQUIREMENTS

1. Alert any personnel in the lab that the laser will be used. All personnel in the lab must either don $CO_2$ laser goggles or exit the lab prior to enabling the water-cooled shutter.
2. Turn ON the "Laser in Use" light outside the laboratory door.
3. Minimize and/or block potential beam reflections.
4. Minimize sample size and distance from beam exit to sample location.

## V. LASER STARTUP PROCEDURE

1. Inspect the beam path – minimize, and if necessary, use the beam dump. Use the red guide beam to ensure the path is unobstructed and incident on the target as desired.
2. Initiate water flow to the $CO_2$ laser (2 GPM). Verify no water leaks along line or near drain.
3. Initiate water flow to the shutter/power meter (~1 to 1.2 GPM), if installed.
4. Plug in the laser at the wall outlet. The green light on the laser power supply will energize.
5. Turn on the laser power supply (key). Amber light on power supply and laser will energize.
6. Turn on the "tickle" switch (located on the switchbox connected to the Kern Electronics laser controller on top of the laser RF power supply) -- the red TICKLE light will energize.
7. When ready to initiate the experiment, ensure the laser switch (on top of the laser near the beam exit is ON. The switch is spring loaded so it will have to be held in the ON position while firing, otherwise it will turn off. Then turn on the "Laser" switch on the switchbox -- the red LASER light on the switchbox will energize and fire the laser immediately.
8. If necessary, adjust the laser output power with the knob on the Kern Electronics laser controller. The power output may be read from the power meter gauge. Keep the water-cooled shutter disabled (closed) during this process.

## VI. LASER SHUTDOWN PROCEDURE

1. Turn OFF the laser (switch over the beam exit).
2. Close the water-cooled shutter via the shutter control module.
3. Turn OFF the “tickle” and “laser” switches.
4. Turn OFF the laser power supply (key).
5. Unplug the laser power supply from the wall outlet.
6. Shutoff shutter/power meter and $CO_2$ laser water supplies (once the system has been allowed to cool).
7. Turn OFF red guide beam.
8. Turn OFF power strip.
9. Turn OFF the “Laser in Use” light outside the laboratory door.

**Combustion Experiment Procedures**

1. Setup the sample and prepare the sample ignition experiment: alignment, oven temp, sample in the center view of the camera, wooden block upright, copper block between oven, TC below sample.
2. Take a calibration shot with camera and scale for each new day of testing or if camera position/settings are changed.
3. Close the furnace and set to the desired preheat temperature. Once the sample has reached desired temperature, allow the sample to soak for 10 min, or until the internal sample TC is at the desired temperature.
4. Put on $CO_2$ safety glasses/goggles.
5. Start-up laser following the laser SOP.
6. Ensure the proper camera settings (Hold is checked on Sampling Rate and Exposure). Open a new sequence in the camera software.
7. Switch both the front shutter switch, near the front of the laser, and the tickle switch to their ON positions.
8. Start the camera by pressing record and DAQ recording BEFORE lasing.
9. While holding the front shutter switch in its ON position, turn the laser control switch ON to fire.
10. Release the front shutter switch when ignition is achieved, then turn shutter, tickle, and laser to their OFF positions. Shut down the laser following the laser SOP.
11. Stop the recording AFTER the burn is complete and verify the camera data file was properly saved as a JPEG Quality 95. Export the full sequence to an avi file.
12. Mention any particular comments about the run.

**Data Processing Procedure**

1. Follow relevant mixing, laser operation, and testing procedures to capture reaction video.
2. Use a USB drive to move the video from the lab testing computer to the work PC with network connection.
3. Record batch and sample parameters in Batch to Checkout.&.Sample Information Excel sheet.

4. Record sample and test parameters in Testing Summary Excel sheet.
5. Open the video file in ImageJ as a “Virtual Stack”.
6. Trim the video to only ignition and flame propagation by using Image->Stacks->Tools->**Slice Remover.** Save the trimmed video in the Video shared folder.
7. Open the calibration image in ImageJ to determine the pixel/distance ratio. Set the ratio for the video file under Analyze->**Set Scale.**
8. Go to Analyze->Set Measurements and check only Centroid and Stack Position.
9. Use the Wand Tracing Tool to select the front center of the flame propagation wave. Press CTRL+M to take a measurement. Continue taking propagation measurements approximately every 10-20 frames until the end of the propagation.
10. In the measurement window, save the measurement data as a csv in the project folder.
11. Open Kaleidagraph and paste the measurement data into the data window.
12. Calculate the time at each frame in the formula window using the camera Frame Rate.
    a. Time = Frame/Frame Rate
13. Plot the x-position with respect to time using Gallery->Linear->Scatter.
14. Fit a line to the scatter with Curve Fit->Linear. The equation of the line appears at the top of the graph and the slope is the flame propagation speed. Record the propagation speed on the Testing Summary sheet.
15. Save the sample Kaleidagraph graph in the QPC Sample Plots folder.

## BIBLIOGRAPHY

[1] R. F. Sawyer, "Science based policy for addressing energy and environmental problems," *Proc. Combust. Inst.*, vol. 31, no. 1, pp. 45–56, 2009, doi: 10.1016/j.proci.2008.07.003.

[2] T. Wilberforce, A. G. Olabi, E. T. Sayed, K. Elsaid, and M. A. Abdelkareem, "Progress in carbon capture technologies," *Sci. Total Environ.*, vol. 761, p. 143203, 2021, doi: 10.1016/j.scitotenv.2020.143203.

[3] J. Adanez, A. Abad, F. Garcia-Labiano, P. Gayan, and L. F. De Diego, "Progress in chemical-looping combustion and reforming technologies," *Prog. Energy Combust. Sci.*, vol. 38, pp. 215–282, 2012, doi: 10.1016/j.pecs.2011.09.001.

[4] L. F. De Diego *et al.*, "Development of Cu-based oxygen carriers for chemical-looping combustion," *Fuel*, vol. 83, pp. 1749–1757, 2004, doi: 10.1016/j.fuel.2004.03.003.

[5] J. Adánez, L. F. De Diego, F. García-Labiano, P. Gayán, A. Abad, and J. M. Palacios, "Selection of oxygen carriers for chemical-looping combustion," *Energy and Fuels*, vol. 18, no. 2, pp. 371–377, 2004, doi: 10.1021/ef0301452.

[6] H. Leion, A. Lyngfelt, M. Johansson, E. Jerndal, and T. Mattisson, "The use of ilmenite as an oxygen carrier in chemical-looping combustion," *Chem. Eng. Res. Des.*, vol. 86, pp. 1017–1026, 2008, doi: 10.1016/j.cherd.2008.03.019.

[7] Y. Cao, B. Casenas, and W. P. Pan, "Investigation of chemical looping combustion by solid fuels. 2. Redox reaction kinetics and product characterization with coal, biomass, and solid waste as solid fuels and CuO as an oxygen carrier," *Energy and Fuels*, vol. 20, no. 5, pp. 1845–1854, 2006, doi: 10.1021/ef050424k.

[8] H. Leion, T. Mattisson, and A. Lyngfelt, “Solid fuels in chemical-looping combustion,” *Int. J. Greenh. Gas Control*, vol. 2, pp. 180–183, 2008, doi: 10.1016/S1750-5836(07)00117-X.

[9] L. Shen, J. Wu, and J. Xiao, “Experiments on chemical looping combustion of coal with a NiO based oxygen carrier,” *Combust. Flame*, vol. 156, pp. 721–728, 2009, doi: 10.1016/j.combustflame.2008.08.004.

[10] P. Markström, C. Linderholm, and A. Lyngfelt, “Chemical-looping combustion of solid fuels - Design and operation of a 100kW unit with bituminous coal,” *Int. J. Greenh. Gas Control*, vol. 15, pp. 150–162, 2013, doi: 10.1016/j.ijggc.2013.01.048.

[11] J. Adanez, A. Abad, T. Mendiara, P. Gayan, and L. F. de Diego, “Chemical looping combustion of solid fuels,” *Prog. Energy Combust. Sci.*, vol. 65, pp. 6–66, 2018.

[12] T. Mattisson, A. Lyngfelt, and H. Leion, “Chemical-looping with oxygen uncoupling for combustion of solid fuels,” *Int. J. Greenh. Gas Control*, vol. 3, pp. 11–19, 2009, doi: 10.1016/j.ijggc.2008.06.002.

[13] R. Siriwardane *et al.*, “Chemical-Looping Combustion of Coal with Metal Oxide Oxygen Carriers,” *Energy and Fuels*, vol. 23, no. 8, pp. 3885–3892, 2009, doi: 10.1021/ef9001605.

[14] Y. Cao and W. P. Pan, “Investigation of chemical looping combustion by solid fuels. 1. Process analysis,” *Energy and Fuels*, vol. 20, no. 5, pp. 1836–1844, 2006, doi: 10.1021/ef050228d.

[15] R. Siriwardane, H. Tian, D. Miller, G. Richards, T. Simonyi, and J. Poston, “Evaluation of reaction mechanism of coal-metal oxide interactions in chemical-looping combustion,” *Combust. Flame*, vol. 157, no. 11, pp. 2198–2208, 2010, doi:

10.1016/j.combustflame.2010.06.008.

[16] J. S. Dennis and S. A. Scott, “In situ gasification of a lignite coal and CO 2 separation using chemical looping with a Cu-based oxygen carrier,” *Fuel*, vol. 89, no. 7, pp. 1623–1640, 2010, doi: 10.1016/j.fuel.2009.08.019.

[17] Garcia-Labiano, L. F. De Diego, J. Adanez, A. Abad, and P. Gayan, “Reduction and Oxidation Kinetics of a Copper-Based Oxygen Carrier Prepared by Impregnation for Chemical-Looping Combustion,” *Ind. Eng. Chem. Res.*, vol. 43, no. 2, pp. 8168–8177, 2004, doi: 10.1021/ie0493311.

[18] S. Y. Chuang, J. S. Dennis, A. N. Hayhurst, and S. A. Scott, “Kinetics of the Oxidation of a Co-precipitated Mixture of Cu and Al 2 O 3 by O 2 for Chemical-Looping Combustion,” *Energy and Fuels*, vol. 24, no. 4, pp. 3917–3927, 2010, doi: 10.1021/ef1002167.

# JARRED G. VASINKO
# ACADEMIC VITA

Jarred.vasinko@comcast.net

## Education

The Pennsylvania State University – B.S. in Mechanical Engineering - 2021
Schreyer Honors College

Thesis Title: "Self-Propagating Chemical-Looping Combustion of Solid Carbon Fuel with Copper Oxide"
Thesis Supervisor: Dr. Richard Yetter

## Professional Experience

Penn State Combustion Research Lab – *Undergraduate Researcher* – 2020 – State College, PA

- Researched chemical-looping combustion processes to simplify $CO_2$ capture during energy production.
- Simulated CLC solid fuel reaction to study flame propagation over varying conditions.

Marathon Petroleum Corporation – *Pipeline Engineering Co-op* – 2020 – La Palma, CA

- Managed pipeline maintenance projects to prevent hazardous pipeline failure.
- Developed piping plans and flow calculations for petroleum pipeline networks.

Marathon Petroleum Corporation – *Pipeline Integrity Co-op* – 2019 – Findlay, OH

- Led in-line inspections and pipeline construction and maintenance projects nationwide.
- Developed an understanding of ASME and API pipping standards and processes for petroleum applications.

L&S Machine Company – *Continuous Improvement Engineer* – 2019 – Latrobe, PA

- Executed Industry 4.0 and LEAN manufacturing solutions for production improvement.
- Programmed and implemented robotics, additive manufacturing, advanced manufacturing equipment.

Diversified Industrial Rigging – *Engineering Intern* – 2019 – Lynchburg, VA

- Designed and evaluated rigging equipment and steel structures using AISC and ASME standards.
- Developed lift plans for complex construction projects.

## Honors and Awards

- UPS James E. Casey National Merit Scholarship
- ASME IGTI Gas and Turbomachinery Scholarship
- Penn State Academic Excellence Scholarship
- ASME Allen Rhodes Memorial Scholarship
- Penn State President's Freshman Award
- Penn State Deans List all four undergraduate years

## Skills and Certifications

- CAD/FEA: SolidWorks, AutoCAD, Autodesk Inventor
- Programming: MATLAB, Arduino, UR Robotics PolyScope
- Certified Haas CNC Operator